Complete momentum balance in ionization of H_2 by 75-keV-proton impact for varying projectile coherence

S. Sharma,[1] T. P. Arthanayaka,[1] A. Hasan,[1,2] B. R. Lamichhane,[1] J. Remolina,[1] A. Smith,[1] and M. Schulz[1]
[1]*Department of Physics and LAMOR, Missouri University of Science & Technology, Rolla, Missouri 65409, USA*
[2]*Department of Physics, UAE University, P. O. Box 15551, Al Ain, Abu Dhabi, United Arab Emirates*
(Received 5 February 2014; published 8 May 2014)

We report on a kinematically complete experiment on ionization of H_2 by proton impact. While a significant impact of the projectile coherence properties on the scattering-angle dependence of double-differential cross sections (DDCSs), reported earlier, is confirmed by the present data, only weak coherence effects are found in the electron and recoil-ion momentum dependence of the DDCSs. This suggests that the phase angle in the interference term is determined primarily by the projectile momentum transfer rather than by the recoil-ion momentum. We therefore cannot rule out the possibility that the interference observed in our data is not primarily due to a two-center effect.

DOI: 10.1103/PhysRevA.89.052703 PACS number(s): 34.50.Fa, 34.50.Bw

I. INTRODUCTION

The dynamics of atomic fragmentation processes has been studied extensively in order to advance our understanding of the fundamental few-body problem, e.g., [1,2]. Measurements of fully differential cross sections (FDCSs) for ionization of simple target atoms or molecules by charged-particle impact have proven to be particularly important as they offer the most sensitive test of theoretical models, e.g., [1–13]. For electron impact, these studies have significantly deepened our insight into the reaction dynamics, which can be quite complex even for simple systems containing only three or four particles. Several sophisticated models have been developed and over the last decade significantly improved agreement with experimental data was achieved e.g., [1,8,14], even close to threshold, which was considered to be a particularly difficult regime.

For ion-impact FDCS measurements are much more challenging due to the larger projectile mass compared to electrons. As a result, the literature on such experiments e.g., [2,9–13], is not as extensive yet. Nevertheless, these studies provided some important new insights complementary to those obtained from electron-impact studies. In particular, a surprisingly strong role played by the nucleus-nucleus (NN) interaction was uncovered e.g., [2,9,15]. However, the agreement with theory was much less satisfactory than for electron impact e.g., [16–19]. It was particularly sobering that significant discrepancies were found even for collision systems with very small perturbation parameter η (the projectile charge-to-speed ratio) [2]. In this regime it was previously taken for granted that even the first Born approximation (FBA) would provide an adequate description of the reaction dynamics. But even state-of-the-art calculations, which diligently account for the NN interaction, did not reproduce the measured FDCSs e.g., [16–19] and it was difficult to see where these sophisticated models could go so severely wrong.

After a decade of vivid debates we presented an experimental study which suggests that this puzzle may be resolvable by properly accounting for the coherence properties of the projectile beam realized in the experiment [20]. Double-differential cross sections (DDCSs) for ionization of H_2 by proton impact were measured for fixed projectile energy loss ε as a function of scattering angle θ. In the experiment the transverse projectile coherence length Δr was changed by placing a collimating slit of fixed width at a variable distance before the target. Since the beam was incoherent without the slit, the transverse coherence length was given by $\Delta r = (L/2a)\lambda$ [21], where a and L are the width of the slit and its distance to the target, respectively, and λ is the de Broglie wavelength of the projectiles. The factor 1/2 in the relation for Δr occurs when the deflected projectiles are analyzed in only one direction [21] (the horizontal direction in our case). The experiment was performed for two different L, one corresponding to $\Delta r > D$, resulting in a coherent beam, and the other to $\Delta r < D$, resulting in an incoherent beam, where D is the internuclear distance of the molecule. In the former case an interference structure was observed, which was absent in the latter case. The same feature was later also observed in the capture channel for the same collision system [22]. The same basic idea of studying such coherence effects was also used in [21], where diffraction of very slow meta-stable Ar atoms from a periodic potential was investigated. However, there Δr was varied by changing a rather than L.

In [20] we further argued that for atomic targets interference between first- and higher-order amplitudes can be present, but that here too, they would be observable only for a coherent projectile beam. Indeed, such interference effects were found in theoretical calculations [23,24]. Since the coherence length of the massive and very fast projectile in [2] was tiny compared to the target size, this could explain the puzzling discrepancies between theory and experiment. Experimental support for this interpretation was indeed obtained [25,26].

In a recent paper Feagin and Hargreaves acknowledged that our data of [20] demonstrate a projectile coherence effect; however, they argued that this should not be viewed as wave packet (de)coherence [27]. Without making any implications about the validity of this statement, we note that in [21] the same effect as observed in our data was actually interpreted as a wave packet (de)coherence effect. Feagin and Hargreaves, on the other hand, asserted that the different DDCSs measured for different collimating slit distances could be reconciled by averaging the cross sections for a fully coherent beam over the angular range subtended by the collimating slit at the target. They further argued that if the momentum vectors of all three collision fragments were measured the scattering angle could be determined from the direct projectile-momentum measurement and from the sum momentum of the electron and the recoil ion. By selecting only events for which both angles are the same (within a small margin) the effective local collimation angle that the slit subtends at the target location should then be significantly decreased, and the differences in the DDCSs measured for a large and a small slit distance should be eliminated or at least strongly reduced.

In this article we report a study of ionization of H_2 by 75-keV-proton impact in which all three momentum components of the scattered projectiles and of the recoiling target ions were measured. Although the ejected electron momentum was not directly measured, the kinematics was nevertheless overdetermined since out of the nine final-state momentum components only five are independent due to the kinematic conservation laws. We therefore not only obtained the complete electron momentum vector, but were also able to determine θ from the direct projectile measurement and independently from the momenta of the target fragments, as suggested in [27]. From the data we draw two important conclusions: (a) The phase angle in the interference term does not seem to be primarily determined by the recoil-ion momentum, as assumed previously, but rather by the projectile momentum transfer. (b) At least part of the analysis by Feagin and Hargreaves of the role of projectile coherence is not supported by our data. However, the data do not provide evidence that their assertion, that any coherence effect should not be interpreted as wave packet (de)coherence, is incorrect and throughout this article we do not use any vocabulary relating to coherence in the context of wave packets.

II. EXPERIMENT

The experiment was performed at Missouri University of Science and Technology. A proton beam was generated with a hot-cathode ion source and extracted through an anode aperture with a diameter of 0.5 mm. The beam was focused by an electrostatic lens, collimated by a second aperture 1.5 mm in diameter and located about 45 cm from the lens, and accelerated to 75 keV. The proton beam was then further collimated in the x direction with a vertical slit of width 150 μm located approximately 150 cm from the aperture and placed at a variable distance from the target. A second slit, oriented horizontally, used to collimate the beam in the y direction (also with a width of 150 μm), was kept at a fixed distance from the target (a few millimeters from the large-distance location of the x slit). In the target chamber the projectile beam intersected with a cold ($T < 2$ K) neutral H_2 beam. The projectiles which were not charge exchanged in the collision were selected by a switching magnet, decelerated to an energy of 5 keV, energy analyzed using an electrostatic parallel-plate analyzer [28] with an energy resolution of 3 eV full width at half maximum (FWHM), and detected by a two-dimensional position sensitive multichannel-plate (MCP) detector. The entrance and exit slits of the analyzer are narrow (75 μm) in the y (vertical) direction, but long (2.5 cm) in the x (horizontal) direction. Therefore, the y component of the momentum transfer $\mathbf{q}$ from the projectile to the target was fixed at 0 (within the experimental resolution) and the projectile position spectrum provided q_x and thereby the projectile scattering angle θ. The z component (defined by the initial projectile beam direction) is given by the projectile energy loss ε as $q_z = \varepsilon / v_p$. The resolution in the x, y, and z components of $\mathbf{q}$ was 0.32, 0.2, and 0.07 a.u. FWHM, respectively.

The recoiling $H_2{}^+$ ions produced in the collision were extracted by a weak electric field (8 V/cm) pointing in the x direction and momentum analyzed by a cold-target recoil-ion-momentum spectrometer (COLTRIMS) (for a detailed description see [29]). The momentum resolution in the x, y, and z directions was 0.15, 0.6, and 0.15 a.u. FWHM, respectively. Since the resolution in the y direction is mainly due to the target temperature it provides an estimate of the initial target momentum, which is negligible compared to the projectile momentum. The projectile and recoil-ion detectors were set in coincidence and the data recorded in event-by-event list mode. The electron momentum was deduced in the data analysis from momentum conservation. The electron energy spectrum, calculated from the electron momentum, reveals a pronounced maximum with a centroid which agrees within 0.5 eV with $\varepsilon - I$, where I is the ionization potential of H_2. A condition on this peak in the energy spectrum was used to further clean the data from any background which may have survived the coincidence-time condition.

The experiment was done for two different slit distances $L = 50$ and 6.5 cm. The larger distance corresponds to a transverse coherence length of 3.3 a.u. For the smaller value the relation between Δr and the slit geometry would suggest a coherence length of 0.43 a.u. However, it should be noted that the collimating slit can only increase but not decrease Δr, an important point which we neglected in [20]. The collimating aperture after the source results in $\Delta r < 1$ a.u. with the collimation slit taken out, which we take as the transverse coherence length at the target location for the slit position closer to the target. For the larger L value $\Delta r > D$, making the beam coherent over the dimension of the molecule ($D = 1.4$ a.u.), while for the smaller L value $\Delta r < D$, corresponding to an incoherent beam. With a smaller extraction voltage on the ion source we have achieved a projectile energy resolution of less than 1 eV FWHM, which provides an upper limit of the intrinsic energy spread ΔE. This yields a lower limit for the longitudinal coherence length $\Delta z \approx (2\Delta p_z)^{-1} = v/2\Delta E = 24$ a.u., so that longitudinal coherence is realized independently of the slit distance.

III. RESULTS AND DISCUSSION

In Fig. 1 the DDCSs for $\varepsilon = 30$ eV are plotted as a function of θ. Here and in all following spectra closed circles represent data taken for large L and open circles data taken for small L. There are some differences from the data of [20] at $\theta > 0.8$ mrad due to the energy condition, mentioned in the Experimental section, which in the present data removed any background at large angles which may have survived the coincidence condition and which could not be applied in Ref. [20]. In this sense the present experiment, being kinematically complete, can be regarded as “cleaner.” This background does not play any role at all at smaller angles, where the cross section is much larger. It should also be noted that the absolute overall

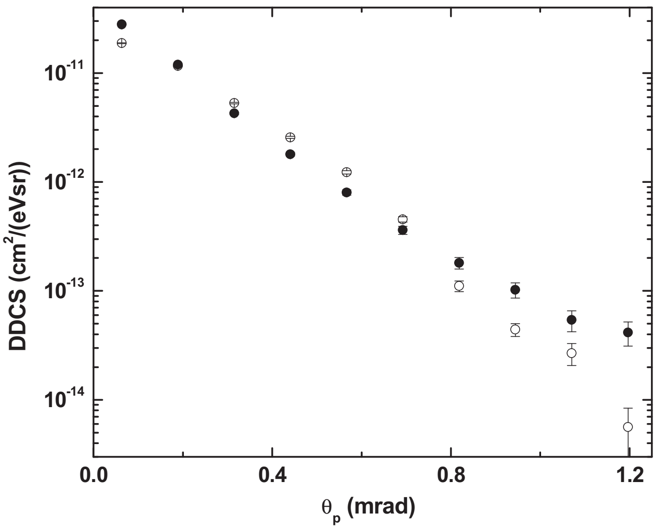

FIG. 1. DDCSs for a fixed energy loss of 30 eV as a function of the projectile scattering angle θ. The closed and open data points were taken for the large and small slit distances, respectively.

magnitude differs by about 50% because the DDCSs of [20] were normalized to $d\sigma/dE_{\mathrm{el}}$ obtained from a semiempirical formula by Rudd *et al.* [30], while the present DDCSs were normalized following the procedure of Alexander *et al.* [31]. Apart from these two differences, the present results are consistent with those reported in [20], i.e., once again we observe significant differences between the DDCSs for a coherent ($\mathrm{DDCS_{coh}}$) and an incoherent ($\mathrm{DDCS_{inc}}$) projectile beam.

Before we analyze the projectile-differential data in more detail we first turn to the recoil-ion and electron momentum spectra. In Fig. 2 the DDCSs for $\varepsilon = 30$ eV are shown as a function of the x components (i.e., the components in the direction of the transverse momentum transfer) of the recoil-ion momentum $p_{\mathrm{rec}x}$ (top panel) and of the electron momentum $p_{\mathrm{el}x}$ (bottom panel). In Fig. 3 we present the DDCSs as a function of the y component of the electron momentum $p_{\mathrm{el}y}$, which (since $q_y = 0$) has the same shape as the $p_{\mathrm{rec}y}$ dependence. Finally, in Fig. 4 the corresponding spectra are plotted for the z components of the recoil-ion and electron momenta.

All electron momentum components (and $p_{\mathrm{rec}y} = -p_{\mathrm{el}y}$) are restricted by the fixed ejected electron energy of 14.6 eV to the range -1.04 to $+1.04$ a.u. This also restricts the kinematically allowed range for the z component of the recoil-ion momentum, given by $p_{\mathrm{rec}z} = q_z - p_{\mathrm{el}z} = \varepsilon/v_p - p_{\mathrm{el}z}$, to -0.4 to 1.7 a.u. In all momentum spectra essentially no counts were observed outside these kinematically allowed regions, except for small contributions due to and within the experimental resolution. Furthermore, the spectrum for $p_{\mathrm{el}y}$ is symmetric about 0, which is a symmetry required by the fact that neither $\mathbf{q}$ nor $\mathbf{v_p}$ has a nonzero y component. These features observed in the data illustrate that the conditions on the coincidence-time peak, on the electron energy calculated from their momentum components, and on the projectile and recoil-ion position spectra removed essentially all of the background from the data.

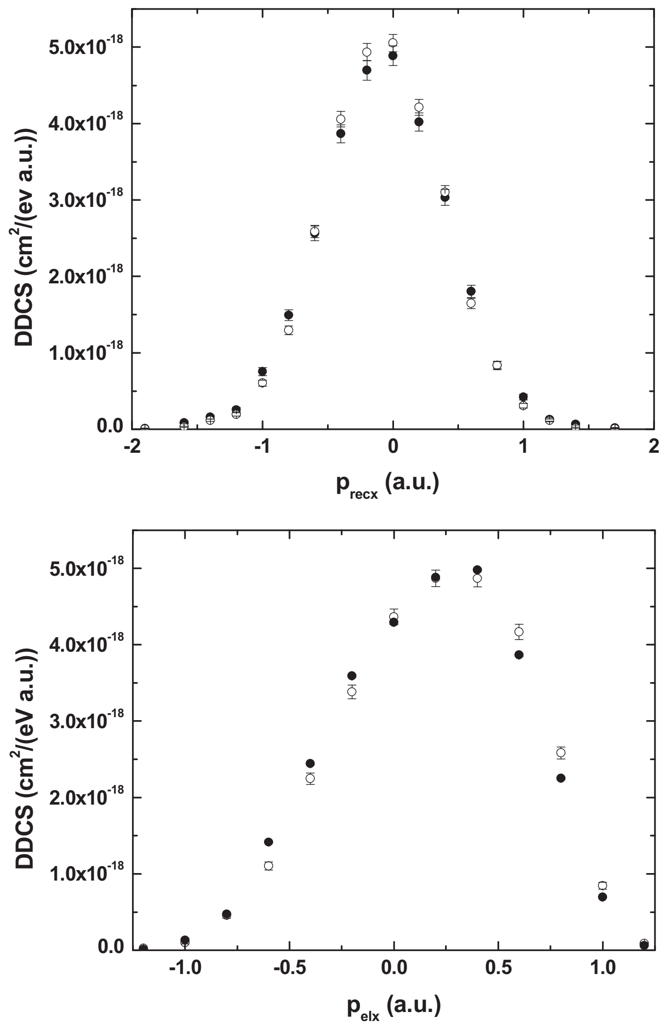

FIG. 2. DDCSs for a fixed energy loss of 30 eV as a function of the x component of the recoil-ion (top) and electron (bottom) momentum. The closed and open data points were taken for the large and small slit distances, respectively.

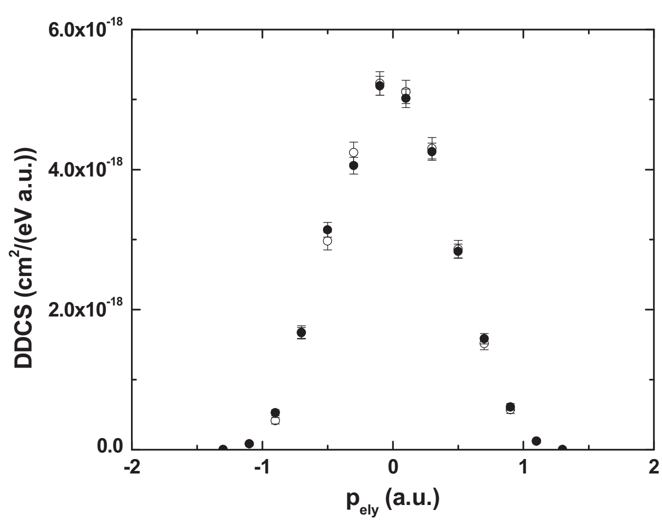

FIG. 3. DDCSs for a fixed energy loss of 30 eV as a function of the y component of the electron. The closed and open data points were taken for the large and small slit distances, respectively.

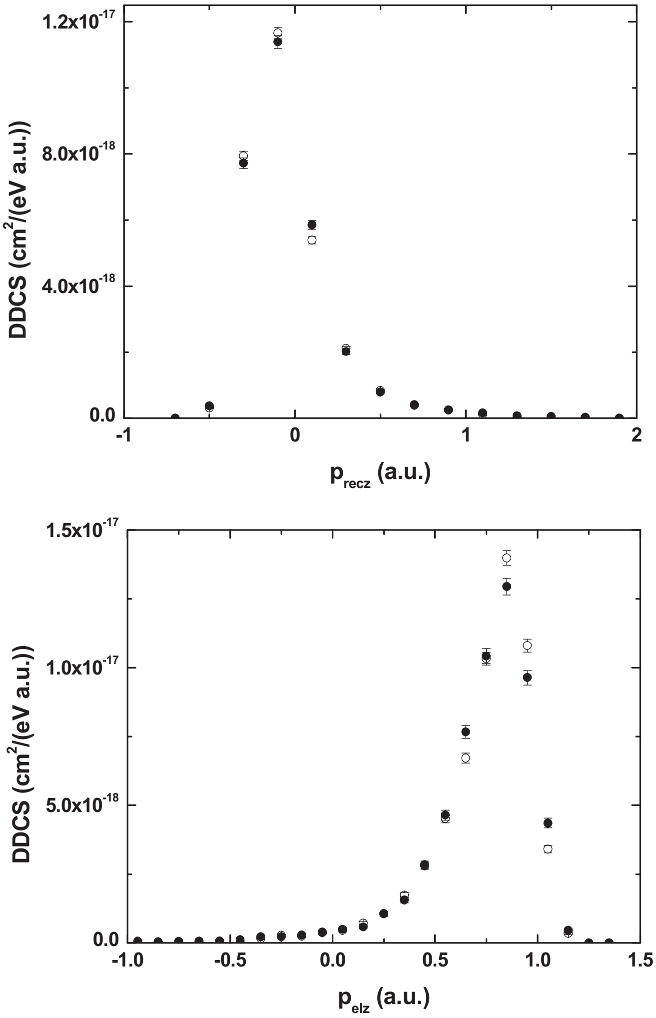

FIG. 4. DDCS for a fixed energy loss of 30 eV as a function of the z component of the recoil-ion (top) and electron (bottom) momentum. The closed and open data points were taken for the large and small slit distances, respectively.

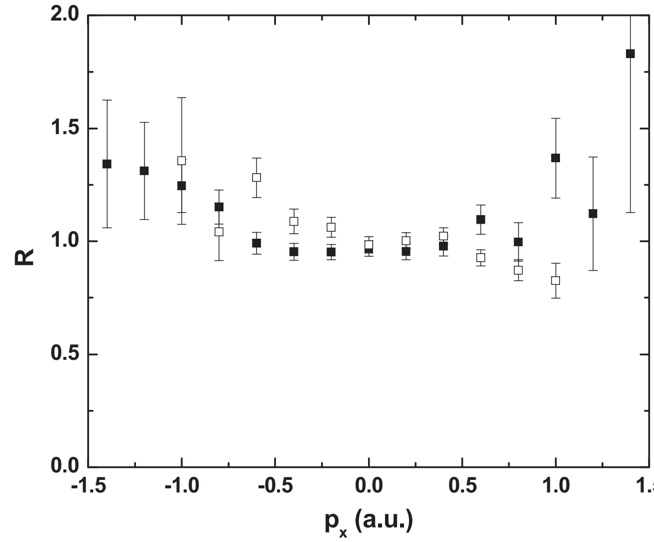

FIG. 5. Ratio between the DDCSs of Fig. 2 for large and small slit distances for the electrons (open symbols) and recoil ions (closed symbols).

For both the electrons and the recoil ions, the coherent and incoherent momentum spectra for the x component look very similar. However, a closer inspection shows that for the electrons the coherent cross sections are systematically larger for $p_{elx} < 0$ and smaller for $p_{elx} > 0.5$ than the incoherent cross sections. Likewise, for the recoil ions the coherent data lie systematically above the incoherent data for $|p_{recx}| > 0.5$ a.u. and below the incoherent data for $|p_{recx}| < 0.5$ a.u. However, in both cases the differences between DDCS_{coh} and DDCS_{inc} are much smaller than in the θ-dependent cross sections.

As outlined in [20] the ratio R between DDCS_{coh} and DDCS_{inc} represents the interference term, which is plotted as a function of p_{elx} (open squares) and p_{recx} (closed squares) in Fig. 5. As seen already in the comparison between DDCS_{coh} and DDCS_{inc} there is only a small departure from $R = 1$. In the corresponding ratios for the DDCSs as a function of the y and z components of the electron and recoil-ion momenta no statistically significant differences from $R = 1$ were observed at all. On the other hand if R is analyzed as a function of the sum momentum $p_{elx} + p_{recx}$, i.e., as a function of q_x, then a pronounced interference structure is observed, as we reported already in [20]. In Fig. 6 this ratio is plotted (closed squares) as a function of $\theta = \sin^{-1}(q_x/p_0)$, where p_0 is the initial projectile momentum. The structure is somewhat damped compared to the data of reference [20], which might be due to different focusing properties of the beam in the two experiments. The coherence properties of the beam without the collimating slit can be affected by the focus. Since, as mentioned above, the collimating slit cannot reduce Δr, in the present experiment Δr for the small L may

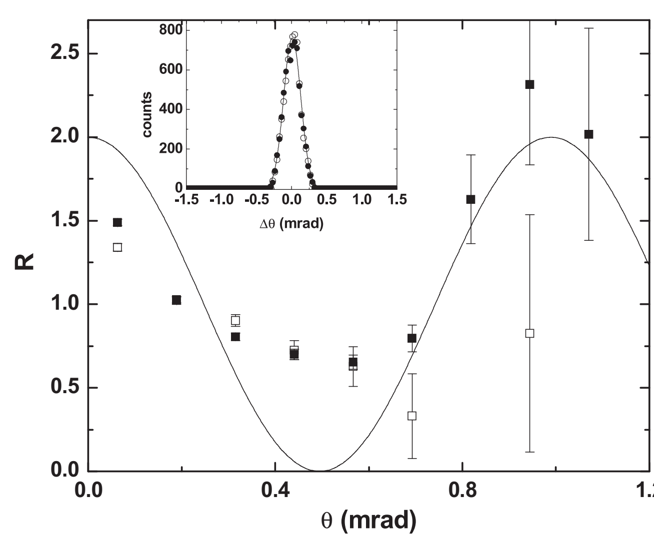

FIG. 6. Ratio between the DDCSs for large and small slit distances as a function of scattering angle (closed symbols). The inset shows DDCSs as a function of the difference between the scattering angles measured directly and determined from the momenta of the target fragments. The open symbols show the ratio with the additional condition $|\Delta\theta| < 0.15$ mrad (see text). The solid line shows the interference term of the form $1 + \cos(q_t \Delta b)$ with $\Delta b = 2$ a.u.

have been slightly larger than in the original experiment. This would be expected to dampen the interference structure in R, as we observe in Fig. 6. However, it should be noted that for both experiments the focus was not changed between the large- and small-slit distance measurements. Apart from these quantitative differences, the qualitative θ dependence of R reported in [20] is reproduced.

The phase angle in the molecular two-center interference term is believed to be determined by $\mathbf{p}_{\rm rec} \cdot \mathbf{D}$ e.g., [32,33]. The observation that the interference structure is rather weak as a function of both $p_{{\rm rec}x}$ and $p_{{\rm el}x}$ but quite pronounced in the q_x dependence suggests that in the present data the phase angle may actually be mostly determined by $\mathbf{q}$ rather than by $\mathbf{p}_{\rm rec}$. This, in turn, could be an indication that the structures we observe in $R(\theta)$ are not primarily due to this type of interference. Another possible explanation for these structures is interference between first-and higher-order ionization amplitudes, which we dub single-center interference. Indeed, as mentioned above, such interference effects have been predicted theoretically e.g., [23,24], and fully differential data for single ionization [25] and transfer ionization [26] for collision systems with atomic targets were interpreted along this line.

Unfortunately, we are not aware of any theoretical analysis providing an expression for the phase angle α leading to single-center interference. We therefore try to estimate α using a simplified semiclassical model. Suppose that $\mathbf{b_1}$ and $\mathbf{b_2}$ are the average impact parameters leading to the same projectile scattering angle θ by the first- and higher-order processes, respectively. The classical projectile trajectories are then separated by $\Delta b = |\mathbf{b_1} - \mathbf{b_2}|$. For a given θ the corresponding diffracted projectile waves reach the detector with a path difference of $d = \Delta b \sin\theta$, which results in $\alpha = (2\pi/\lambda)d = (2\pi/\lambda)\Delta b \sin\theta = q_t \Delta b$, where q_t is the transverse component of $\mathbf{q}$. The interference term is then given by $1 + \cos(q_t \Delta b)$. Of course, without a rigorous treatment of the ionization process Δb cannot be determined. However, b_1 and b_2 are surely of the order of the atomic target size so that a reasonable estimate for Δb (which can be anywhere between $|\mathbf{b_1}| - |\mathbf{b_2}|$ and $|\mathbf{b_1}| + |\mathbf{b_2}|$) is a few a.u. The solid curve in Fig. 6 shows a best fit of the interference term to the measured $R(\theta)$, which yields $\Delta b = 2$ a.u.

This discussion of a potentially important role of single-center interference should not be viewed as a firm conclusion, but rather as one possible explanation of the data which we believe is worth pursuing. However, there are alternative interpretations which should also be investigated. For example, we cannot rule out the possibility that even in two-center molecular interference α is primarily determined by $\mathbf{q}$ since we are not aware of any indisputable experimental evidence to the contrary. A fully differential study of this type of interference was performed for capture in $H_2{}^+$+He collisions [34] and there the data were consistent with a phase angle given by $\mathbf{p}_{\rm rec} \cdot \mathbf{D} + \pi$. However, kinematically this reaction represents a two-body scattering process so that $\mathbf{p}_{\rm rec} = \mathbf{q}$. On the other hand, fully differential data for ionization of H_2 by electron impact could not be fully explained with the assumption that α is primarily determined by $\mathbf{p}_{\rm rec}$ [35,36]. It is thus not clear yet whether the present data are mostly due to one- or two-center interference (or a combination of both).

Finally, we address the suggestion of Feagin and Hargreaves to plot $R(\theta)$ with the additional condition that θ directly measured and determined from the momenta of the target fragments must agree within a small margin. Although the electron momentum was not directly measured in our experiment, we can nevertheless obtain $p_{{\rm el}x}$ completely independently of q_x because measuring a total of six momentum components makes the data kinematically overdetermined. Applying momentum conservation, we obtain $p_{{\rm el}y}$ and $p_{{\rm el}z}$ from the directly measured $q_{y,z}$ and $p_{{\rm rec}y,z}$. Using energy conservation, $p_{{\rm el}x}$ is then given by $p_{{\rm el}x} = \sqrt{(2E_{\rm el} - p_{{\rm el}y}^2 - p_{{\rm el}z}^2)}$, where $E_{\rm el}$ is $\varepsilon - I$. Along with the directly measured $p_{{\rm rec}x}$ this provides a second independent method of obtaining the transverse momentum transfer, which we label q_x' to distinguish it from the directly measured q_x. Finally, we compute $\Delta\theta = \sin^{-1}(q_x'/p_0) - \sin^{-1}(q_x/p_0)$, which is plotted for the coherent (closed symbols) and incoherent (open symbols) data in the inset of Fig. 6. With infinitely good overall resolution (including the angular spread of the incident projectile beam) this spectrum should be a δ function at 0. The actual spectrum is a perfectly symmetric distribution centered at $\Delta\theta = 0$ within 10 μrad, illustrating a high accuracy in the calibration of the measured momentum components. Using error propagation on the momentum resolutions stated in the experimental section the resolution in $\Delta\theta$ should be 0.27 mrad FWHM, which is in very good accord with the width of the actual spectrum of 0.28 mrad FWHM.

The resolution in $\Delta\theta$ does not differ noticeably for the coherent and incoherent beams. This is a first indication that the prediction of Feagin and Hargreaves is not supported by our results. This is confirmed by $R(\theta)$ generated with the condition $|\Delta\theta| < 0.15$ mrad, which is plotted as open squares in Fig. 3. These data agree very well with $R(\theta)$ without that condition, with the possible exception of the region of large θ. However, considering the large error bars of the data with the condition in this region it is not clear whether these differences are statistically significant. Overall, the structure in $R(\theta)$ is not substantially weakened by the condition on $\Delta\theta$, contrary to the prediction of Feagin and Hargreaves [27]. We do not believe that this result entirely invalidates their analysis, which we regard as a valuable contribution. In particular, we do not discard yet their conclusion that the coherence effects observed in our data are not to be interpreted as wave packet (de)coherence. Further studies are called for to address this important point. However, our results do show that the differences in the cross sections measured with a coherent and an incoherent beam cannot be simply explained by experimental resolution effects.

IV. CONCLUSIONS

In summary, we have confirmed a pronounced projectile coherence effect in the scattering angle dependence of DDCSs for ionization of H_2 by proton impact. Surprisingly, in the recoil-ion momentum (and electron momentum) dependence the coherence effect is significantly weaker. This is an indication that the phase angle in the interference term is primarily determined by $\mathbf{q}$ rather than by $\mathbf{p}_{\rm rec}$. The reason for this unexpected result is presently not clear. Here, we offered two different explanations: first, the previous assumption that the phase factor in molecular two-center interference is determined by $\mathbf{p}_{rec}$ may be incorrect and second, the structures seen in our data may be due to a different type of interference, such as, e.g., interference between first- and higher-order scattering amplitudes.

We also tested the prediction by Feagin and Hargreaves that the differences between the cross sections measured for a coherent and an incoherent beam will disappear if a condition is applied that the scattering angles directly measured from the projectile and determined from the electron and recoil-ion momenta agree with each other within a small margin. Our results do not support this prediction. Rather, we find that the ratio between the cross sections for a coherent and an incoherent beam are hardly affected at all by this condition. Therefore, further analysis is called for to reconcile the theoretical work of Feagin and Hargreaves with our experimental results.

ACKNOWLEDGMENTS

This work was supported by the National Science Foundation under Grant No. PHY-0969299. We are grateful for valuable discussions with many of our friends and colleagues.

[1] T. N. Rescigno, M. Baertschy, W. A. Isaacs, and C. W. McCurdy, Science **286**, 2474 (1999).

[2] M. Schulz, R. Moshammer, D. Fischer, H. Kollmus, D. H. Madison, S. Jones, and J. Ullrich, Nature (London) **422**, 48 (2003).

[3] H. Ehrhardt, M. Schulz, T. Tekaat, and K. Willmann, Phys. Rev. Lett. **22**, 89 (1969).

[4] J. Röder, H. Ehrhardt, I. Bray, D. V. Fursa, and I. E. McCarthy, J. Phys. B **29**, 2103 (1996).

[5] A. J. Murray, M. B. J. Woolf, and F. H. Read, J. Phys. B **25**, 3021 (1992).

[6] M. Dürr, C. Dimopoulou, B. Najjari, A. Dorn, K. Bartschat, I. Bray, D. V. Fursa, Zhangjin Chen, D. H. Madison, and J. Ullrich, Phys. Rev. A **77**, 032717 (2008).

[7] A. Lahmam-Bennani, E. M. Staicu Casagrande, and A. Naja, J. Phys. B **42**, 235205 (2009).

[8] X. Ren, I. Bray, D. V. Fursa, J. Colgan, M. S. Pindzola, T. Pflüger, A. Senftleben, S. Xu, A. Dorn, and J. Ullrich, Phys. Rev. A **83**, 052711 (2011).

[9] N. V. Maydanyuk, A. Hasan, M. Foster, B. Tooke, E. Nanni, D. H. Madison, and M. Schulz, Phys. Rev. Lett. **94**, 243201 (2005).

[10] M. Schulz, R. Moshammer, A. N. Perumal, and J. Ullrich, J. Phys. B **35**, L161 (2002).

[11] R. Hubele, A. LaForge, M. Schulz, J. Goullon, X. Wang, B. Najjari, N. Ferreira, M. Grieser, V. L. B. de Jesus, R. Moshammer, K. Schneider, A. B. Voitkiv, and D. Fischer, Phys. Rev. Lett. **110**, 133201 (2013).

[12] M. Schulz, B. Najjari, A. B. Voitkiv, K. Schneider, X. Wang, A. C. Laforge, R. Hubele, J. Goullon, N. Ferreira, A. Kelkar, M. Grieser, R. Moshammer, J. Ullrich, and D. Fischer, Phys. Rev. A **88**, 022704 (2013).

[13] M. Schulz and D. H. Madison, Int. J. Mod. Phys. A **21**, 3649 (2006).

[14] Z. Chen, D. H. Madison, and K. Bartschat, J. Phys. B **40**, 2333 (2007).

[15] M. Schulz, R. Moshammer, D. Fischer, and J. Ullrich, J. Phys. B **36**, L311 (2003).

[16] D. Madison, M. Schulz, S. Jones, M. Foster, R. Moshammer, and J. Ullrich, J. Phys. B **35**, 3297 (2002).

[17] K. A. Kouzakov, S. A. Zaytsev, Yu. V. Popov, and M. Takahashi, Phys. Rev. A **86**, 032710 (2012).

[18] M. McGovern, C. T. Whelan, and H. R. J. Walters, Phys. Rev. A **82**, 032702 (2010).

[19] M. McGovern, D. Assafrão, J. R. Mohallem, C. T. Whelan, and H. R. J. Walters, Phys. Rev. A **81**, 042704 (2010).

[20] K. N. Egodapitiya, S. Sharma, A. Hasan, A. C. Laforge, D. H. Madison, R. Moshammer, and M. Schulz, Phys. Rev. Lett. **106**, 153202 (2011).

[21] C. Keller, J. Schmiedmayer, and A. Zeilinger, Opt. Commun. **179**, 129 (2000).

[22] S. Sharma, A. Hasan, K. N. Egodapitiya, T. P. Arthanayaka, G. Sakhelashvili, and M. Schulz, Phys. Rev. A **86**, 022706 (2012).

[23] X. Y. Ma, X. Li, S. Y. Sun, and X. F. Jia, Europhys. Lett. **98**, 53001 (2012).

[24] A. B. Voitkiv, B. Najjari, and J. Ullrich, J. Phys. B **36**, 2591 (2003).

[25] X. Wang, K. Schneider, A. LaForge, A. Kelkar, M. Grieser, R. Moshammer, J. Ullrich, M. Schulz, and D. Fischer, J. Phys. B **45**, 211001 (2012).

[26] K. Schneider, M. Schulz, X. Wang, A. Kelkar, M. Grieser, C. Krantz, J. Ullrich, R. Moshammer, and D. Fischer, Phys. Rev. Lett. **110**, 113201 (2013).

[27] J. M. Feagin and L. Hargreaves, Phys. Rev. A **88**, 032705 (2013).

[28] A. D. Gaus, W. Htwe, J. A. Brand, T. J. Gay, and M. Schulz, Rev. Sci. Instrum. **65**, 3739 (1994).

[29] M. Schulz, A. Hasan, N. V. Maydanyuk, M. Foster, B. Tooke, and D. H. Madison, Phys. Rev. A **73**, 062704 (2006).

[30] M. E. Rudd, Y.-K. Kim, D. H. Madison, and T. J. Gay, Rev. Mod. Phys. **64**, 441 (1992).

[31] J. S. Alexander, A. C. Laforge, A. Hasan, Z. S. Machavariani, M. F. Ciappina, R. D. Rivarola, D. H. Madison, and M. Schulz, Phys. Rev. A **78**, 060701(R) (2008).

[32] N. Stolterfoht, B. Sulik, V. Hoffmann, B. Skogvall, J. Y. Chesnel, J. Rangama, F. Frémont, D. Hennecart, A. Cassimi, X. Husson, A. L. Landers, J. A. Tanis, M. E. Galassi, and R. D. Rivarola, Phys. Rev. Lett. **87**, 023201 (2001).

[33] S. E. Corchs, R. D. Rivarola, J. H. McGuire, and Y. D. Wang, Phys. Scr. **50**, 469 (1994).

[34] L. Ph. H. Schmidt, S. Schössler, F. Afaneh, M. Schöffler, K. E. Stiebing, H. Schmidt-Böcking, and R. Dörner, Phys. Rev. Lett. **101**, 173202 (2008).

[35] Z. N. Ozer, H. Chaluvadi, M. Ulu, M. Dogan, B. Aktas, and D. H. Madison, Phys. Rev. A **87**, 042704 (2013).

[36] A. Senftleben, T. Pflüger, X. Ren, O. Al-Hagan, B. Najjari, D. H. Madison, A. Dorn, and J. Ullrich, J. Phys. B **43**, 081002 (2010).